FA-TR-76028

STRESS ANALYSIS OF PALLET LEVER SHAFT

by

Paul F. Gordon
Fee Men Lee
Ramesh Kajaria

March 1976

Approved for public release; distribution unlimited.

Pitman-Dunn Laboratories

U.S. ARMY ARMAMENT COMMAND
FRANKFORD ARSENAL
PHILADELPHIA, PENNSYLVANIA 19137

DISPOSITION INSTRUCTIONS

Destroy this report when it is no longer needed. Do not return it to the originator.

The findings in this report are not to be construed as an official Department of the Army position unless so designated by other authorized documents.

DEPARTMENT OF THE ARMY
FRANKFORD ARSENAL
PHILADELPHIA, PENNSYLVANIA 19137

REPLY TO
ATTENTION OF:

Erratum Sheet for FA Report TR-76028 (March 1976)

TITLE: Stress Analysis of Pallet Lever Shaft

AUTHORS: Paul F. Gordon, Fee M. Lee, Ramesh Kajaria

INTRODUCTION

The effect of the load, Fw, after being transferred from the pin to the shaft, consists of a force of magnitude Fw and a couple (see Fig 4, page 13). This force, Fw, acts on the shaft at the center of the pallet, and its distance M, from point A should be .29 in. instead of the .26 in. used in the subject report (see top of page 10). The revision in the results which this change introduces are given below.

REVISED RESULTS

1. The term M should be replaced by N in equations 9, 10, 15, 16, 21, 22, 27 and 28, and equations 11, 12, 17, 18, 23, 24, 29, 30 should be deleted.

2. The corrected stress calculations show that the maximum combined stresses (table 4 and 5) still occur at the exterior boundary points. In both phase I and II, (see table 1, page 10 and Fig 4 and 5, page 13 and 14) the maximum combined stress occurs at point D for all six cases. The value 95, 91, 89, 141, 121 and 91 ksi replace, in sequence, the values 103, 98, 93, 101, 73 and 49 ksi which were originally given (see table 4 and 5). The net result is that in phase I the maximum combined stresses decrease slightly for all three cases. In phase II the maximum combined stresses increase for all three cases.

3. All graphs showing shear force and moment diagrams in the original report should be deleted.

DISCUSSION AND CONCLUSIONS

The maximum stress found in the elastic analysis with no stress concentration factor was 141 ksi, which exceeded the 120 ksi yield stress of the shaft material. It is concluded that the shaft will fail plastically. Thus the conclusions reached on page 34 of the original report are still completely valid, and on that page the value of the maximum stress of 103 ksi is replaced by 141 ksi. In addition the maximum combined stress is now found in case 1 of phase II, rather than in case 1 of phase I, as given in the original report.

UNCLASSIFIED

SECURITY CLASSIFICATION OF THIS PAGE *(When Data Entered)*

REPORT DOCUMENTATION PAGE

READ INSTRUCTIONS BEFORE COMPLETING FORM

1. REPORT NUMBER: FA-TR-76028	2. GOVT ACCESSION NO.
3. RECIPIENT'S CATALOG NUMBER	
4. TITLE *(and Subtitle)*: STRESS ANALYSIS OF PALLET LEVER SHAFT	5. TYPE OF REPORT & PERIOD COVERED: Technical Research Report
6. PERFORMING ORG. REPORT NUMBER	
7. AUTHOR(s): PAUL G. GORDON FEE MEN LEE RAMESH KAJARIA	8. CONTRACT OR GRANT NUMBER(s)
9. PERFORMING ORGANIZATION NAME AND ADDRESS: FRANKFORD ARSENAL ATTN: SARFA-PDM-E PHILADELPHIA, PA 19137	10. PROGRAM ELEMENT, PROJECT, TASK AREA & WORK UNIT NUMBERS: AMCMS CODE: 4110.16.4737.6 DA PROJECT: GG 46106
11. CONTROLLING OFFICE NAME AND ADDRESS: FRANKFORD ARSENAL PHILADELPHIA, PA 19137	12. REPORT DATE: March 1976 13. NUMBER OF PAGES: 40
14. MONITORING AGENCY NAME & ADDRESS *(if different from Controlling Office)*	15. SECURITY CLASS. *(of this report)*: UNCLASSIFIED 15a. DECLASSIFICATION/DOWNGRADING SCHEDULE: N/A

16. DISTRIBUTION STATEMENT *(of this Report)*

Approved for public release; distribution unlimited.

17. DISTRIBUTION STATEMENT *(of the abstract entered in Block 20, if different from Report)*

18. SUPPLEMENTARY NOTES

19. KEY WORDS *(Continue on reverse side if necessary and identify by block number)*

Bending stress
Stress concentration factor
Von-Mises theory of failure
Bi-axial bending
Plastic failure
Centrigugal failure
Fuze

20. ABSTRACT *(Continue on reverse side if necessary and identify by block number)*

A stress analysis of the pallet lever shaft in the M125A1 Booster Runaway Assembly has been performed. The loading was such that bending and shear stress calculations in two orthogonal planes were required. Both elastic and plastic flow calculations were performed for the bending analysis. Stress concentrations due to the introduction of the "D" cut, which was machined on the originally circular section, were estimated. The mode of failure was shown to be a ductile, plastic weakening and loss of load carrying capacity.

DD FORM 1 JAN 73 1473 EDITION OF 1 NOV 65 IS OBSOLETE

UNCLASSIFIED

SECURITY CLASSIFICATION OF THIS PAGE *(When Data Entered)*

TABLE OF CONTENTS

LIST OF ILLUSTRATIONS

LIST OF TABLES

GLOSSARY

A - Cross section area, in^2

C_X - Distance from the neutral axis, X', in.

C_Y - Distance from the neutral axis, Y', in.

D - Diameter of shaft, in.

d - Distance between centerline of pallet lever shaft to location where F_W acts, in.

d' - Remaining height of slotted cross section of shaft, in.

d'' - Diameter of grooved cross section of shaft, in.

F_C - Centrifugal force acting on pallet lever shaft, lb_f

F_W - External force acting on pallet lever shaft, lb_f

F_{CX} - Component of F_C acting in the Y direction, lb_f

F_{WX} - Component of F_W acting in the X direction, lb_f

F_{WY} - Component of F_W acting in the Y direction, lb_f

I - Moment of inertia, in^4

$I_{X'}$ - Moment of inertia acting about the neutral axis, X', $in.^4$

$I_{Y'}$ - Moment of inertia acting about the neutral axis, Y', $in.^4$

K_t' - Stress concentration factor for bi-axial bending with Von-Mises theory of failure

k - Yield stress in simple shear, psi

L - Length of shaft, in.

M - Location from left side of shaft where F_W acts, in.

M_c - Critical moment, $in\text{-}lb_f$

M_f - Upper limit of moment for failure, $in\text{-}lb_f$

M_X - Internal bending moment about the X-axis, $in\text{-}lb_f$

M_Y - Internal bending moment about the Y-axis, $in\text{-}lb_f$

M_{WX} - Bending moment about the X-axis at the centerline of the shaft due to F_W, $in\text{-}lb_f$

M_{WY} - Bending moment about the Y-axis at the centerline of the shaft due to F_W, $in\text{-}lb_f$

N - Location from left side of shaft where F_C acts, in.

R - Radius of shaft in Figure 1, in.

R_{AX} - Reaction at end of shaft in the X direction, lb_f

R_{AY} - Reaction at end of shaft in the Y direction, lb_f

R_{DX} - Reaction at end of shaft in the X direction, lb_f

R_{DY} - Reaction at end of shaft in the Y direction, lb_f

r - Radius of groove in shaft, in.

r_o - Radius of outer fiber of shaft, in.

V - Shear force, lb_f

V_x - X component of shear force, lb_f

V_y - Y component of shear force, lb_f

X' - Coordinate as measured from neutral axis in the X direction

Y - Frame of reference, Y-axis

Y' - Coordinate as measured from neutral axis in the Y direction

~~Z~~ - Distance from left end of shaft, in.

ζ - Position of plastic interface, in.

θ - Angle F_W makes with Y-axis, degree

ϕ - Angle F_C makes with X-axis, degree

σ - Normal stress, psi

σ_1 - Bending stress in the Z direction produced by the bending moment about the X-axis, M_X, psi

σ_a - Bending stress in the Z direction produced by the bending moment about the Y-axis, M_Y, psi

σ_{mm} - Combined bending stress of σ_1 and σ_2, psi

σ_y - Tensile yield strength, psi

τ_x - Shear stress, psi

INTRODUCTION

The work described in this report was performed under D. A. (Fuze) Project GG46106, the M125A1 Booster Program. The objective of this program was to provide engineering support during production of the M125A1 booster runaway escapement mechanism. This task dealt with production line failures of the pallet lever shaft of that mechanism. The stress analysis performed under that task in support of the failure analysis is presented in this report.

The function of the pallet lever assembly, Figure 1, is to delay the arming of the M125A1 Booster, Figure 2, until the fuze is a safe distance away from launch. A previous mechanism modification described in Tech report FA-TR-74045[1] necessitated the use of a pallet shaft containing a "D" cut to insure adequate escapewheel clearance in addition to an efficient torque exchange at the escapewheel-pallet contact point. The structural integrity of the shaft design which resulted was questioned when premature arming of the M125A1 Booster was observed in lot acceptance testing with the 90 mm M41 Gun. The spin environment produced by this weapon is nominally 19, 500 rpm and results in a high centrifugal loading on all mechanism components. This also results in a high applied torque on the unbalanced rotor gear which powers the mechanism. This torque is reduced and transmitted to the pallet lever exerting additional force on the pallet shaft.

The magnitude of forces used as input to this stress analysis reflect this 19, 500 rpm spin environment, with the rotor gear taken in a maximum output orientation. No gear train losses were assumed anywhere in the device in computing the force applied by the escapewheel on the pallet lever. Since the pallet lever can assume a wide range or orientations with respect to the centrifugal force field, four positions which span the extremes of both entrance and exit engagement positions are analyzed. It was concluded as a result of this study that the pallet lever shaft was on the verge of excessive ductile, plastic bending. The acceptance lot testing failures exhibited the predicted failure mode.

ANALYSIS

Loads and Reactions on the Shaft

The purpose of the analysis is to determine the normal and shearing stresses in the shaft. However, it is necessary first to determine the loads and reactions which generate the stress system.

The right circular beam under consideration is shown in Figures 1 and 3, together with the prescribed loads. The two separate loading conditions for the placement of F_W are called Phase I (Figure 1) and Phase II (Figure 3). As can be noted,

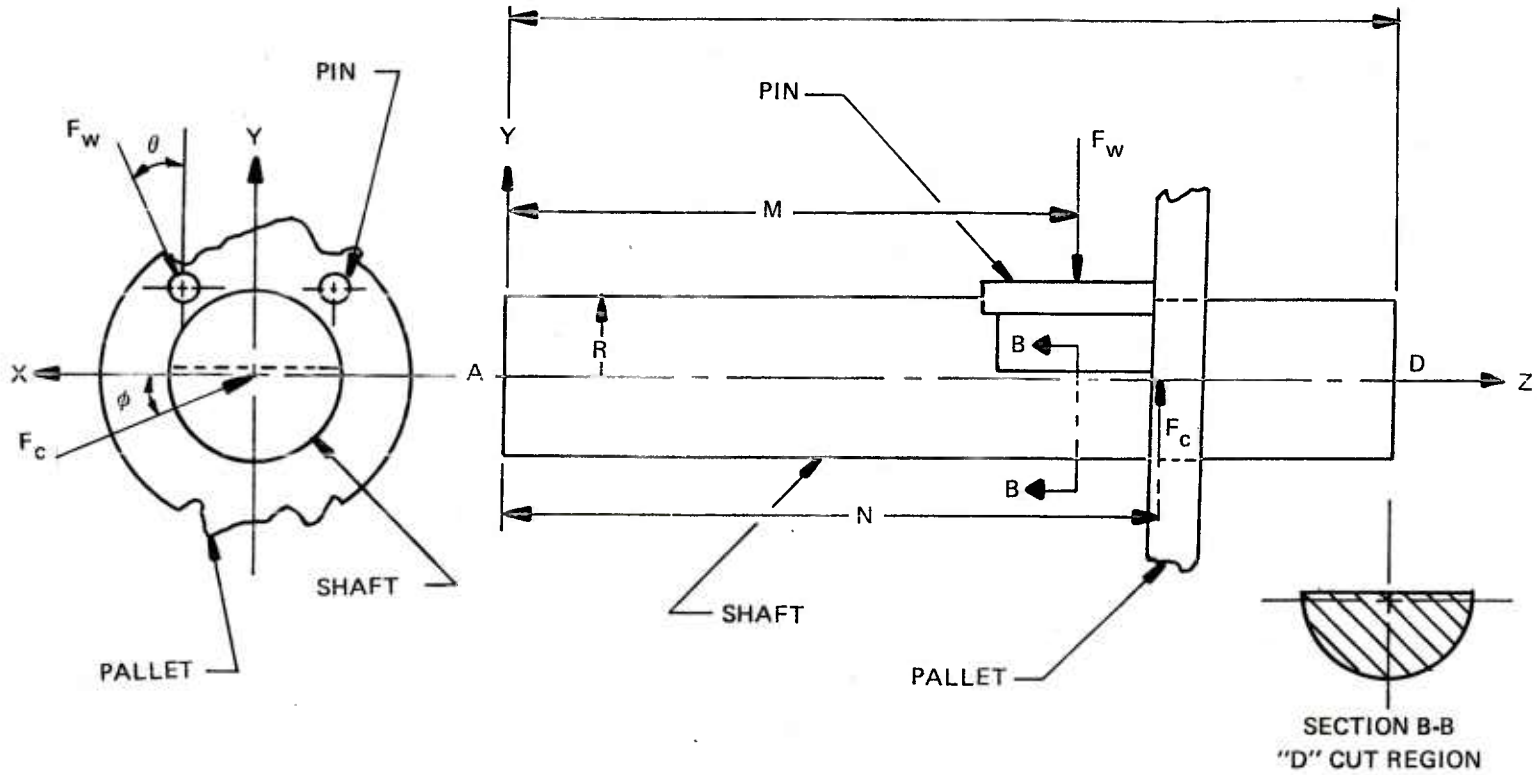

Figure 1. Pallet Lever Assembly (Prescribed Loads for Phase I.)

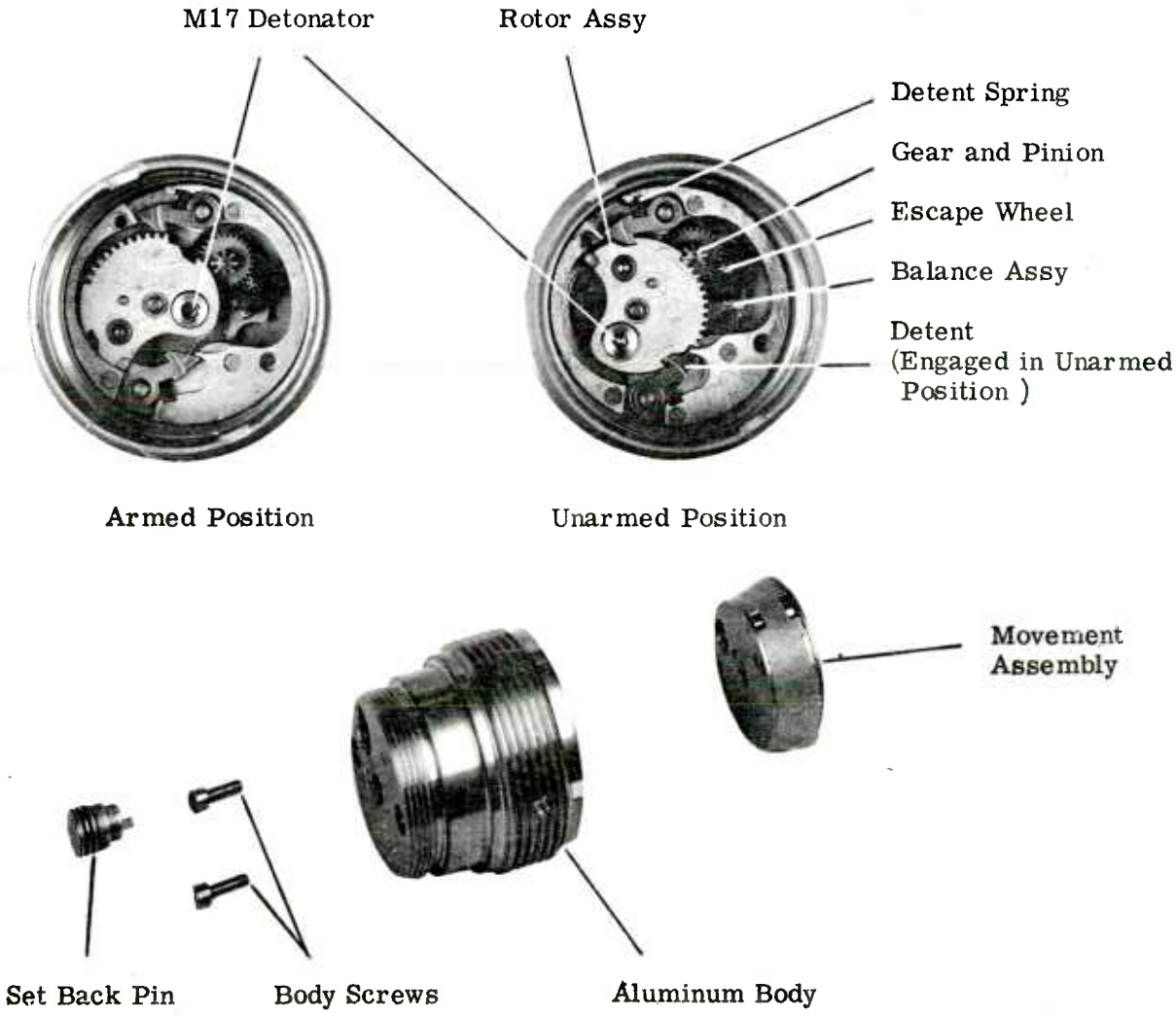

Figure 2. M125A1 Modular Booster

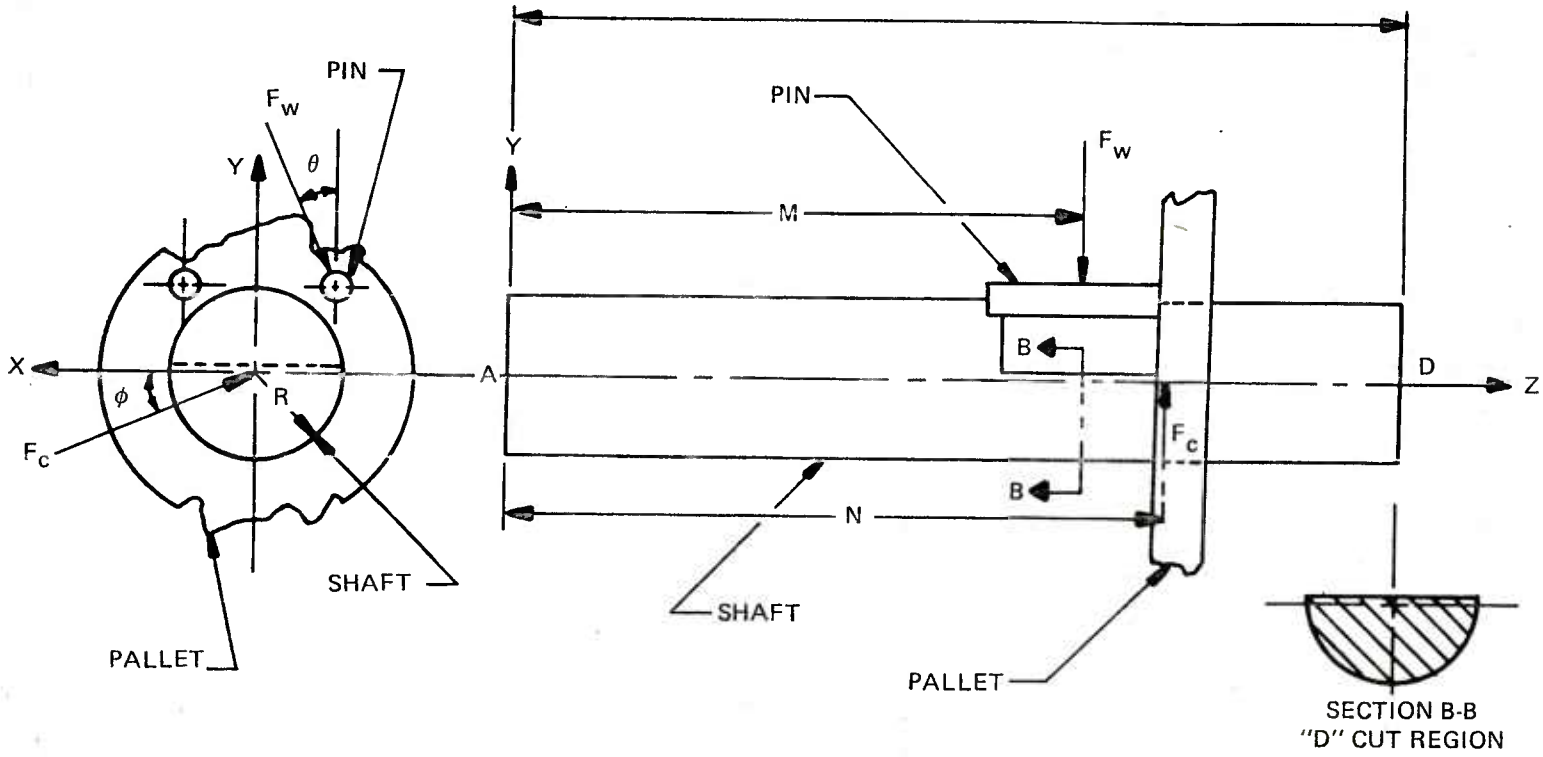

Figure 3. Pallet Lever Assembly (Prescribed Load for Phase II.)

the only difference in the nature of the loading between Phase I and II is the pin and inclination on which F_W acts. Within each phase are three possible values of the loads and inclinations. These three possibilities are identified as cases 2 or 3. The beam was loaded in each Phase by two forces: an external force, F_W, and a centrifugal force, F_C. The dimensions M, N, and L have values of .26 in., .28 in., and .39 in., respectively. Both forces F_W and F_C act in the X-Y plane at inclinations of θ and φ with respect to the Y-axis and X-axis, respectively, and are normal to the Z-axis. Numerical values for the loads and angles are found in Table 1. The external force, F_W, as shown acts on the pin, thus in addition to the usual shear loading, it also contributes a concentrated bending moment to the shaft about the Z-axis at the centerline of the pallet.

For ease in presentation, the components of each force and bending moment in the X-Z and Y-Z planes are illustrated in Figures 4 and 5. Numerical values are listed in Table 2. The reactions (R_{AX}, R_{AY}, R_{DX}, and R_{DY}) were found by demanding static equilibrium in the shaft. The following expressions resulted:

Table 1. Prescribed Loads

Phase I (Figure 1)				
Case	F_W, lb	θ, degrees	F_C, lb	θ, degrees
1	5.78	17	7.4	22
2	4.78	16	7.4	15
3	3.49	18	7.4	5.5
Phase II (Figure 3)				
Case	F_W, lb	θ, degrees	F_C, lb	θ, degrees
1	5.69	30	7.4	-10
2	4.67	39.5	7.4	-5.5
3	3.61	56	7.4	+4

Table 2. X and Y Components of F_W and F_c

Case	F_{WY}, lb	F_{CY}, lb	F_{WX}, lb	F_{CX}, lb
Phase I				
1	5.27	2.77	1.69	6.86
2	4.59	1.98	1.32	7.13
3	3.32	.71	1.08	7.37
Phase II				
1	4.93	1.28	2.84	7.29
2	3.60	1.28	2.97	7.29
3	2.02	.52	2.99	7.38

Phase I:

$$R_{DX} = (F_{CX}N + F_{WX}M - F_{WX}d)/L \quad (1)$$

$$R_{AX} = F_{WX} + F_{CX} - [(F_{CX}N + F_{WX}M - F_{WX}d)/L] \quad (2)$$

$$R_{DY} = (F_{WY}M - F_{CY}N - F_{WY}d)/L \quad (3)$$

$$R_{AY} = F_{WY} - F_{CY} - [(F_{WY}M - F_{CY}N - F_{WY}d)/L] \quad (4)$$

Phase II:

$$R_{DX} = (F_{WX}M + F_{CY}N - F_{WX}d)/L \quad (5)$$

$$R_{AX} = F_{WX} + F_{CY} - [(F_{WX}M + F_{CY}N - F_{WX}d)/L] \quad (6)$$

$$R_{DY} = (F_{WY}M - F_{CY}N - F_{WY}d)/L \quad (7)$$

$$R_{AY} = F_{WY} - F_{CY} - [(F_{WY}M - F_{CY}N - F_{WY}d)/L] \quad (8)$$

Tables 1 and 2 and Figures 1, 3, 4 completely define the system of prescribed loads and resulting reactions. Subsequently, a stress and failure analysis, presented below, was performed using these loads.

The results of this study include (a) an elastic stress analysis, and (b) a plastic stress and failure analysis. The first step in both analyses was the determination of the shear and bending moment diagrams.

Shear and Moment Diagrams

The shear force and bending moment were found to be for Phase I, (Figure 4):

X Component:

$O < Z < M$

$$V_X = - R_{AX} \tag{9}$$

$$M_Y = R_{AX} Z \tag{10}$$

$M < Z < N$

$$V_X = F_{WX} - R_{AX} \tag{11}$$

$$M_Y = R_{AX} Z - F_{WX} (Z - M) \tag{12}$$

$N \quad Z < L$

$$V_X = F_{CX} + F_{WX} - R_{AX} \tag{13}$$

$$M_Y = R_{AX} Z - F_{WX} (Z - M) - F_{CX} (Z - N) - M_{WX} \tag{14}$$

Y Component:

$O < Z < M$

$$V_Y = R_{AY} \tag{15}$$

$$M_X = R_{AY} Z \tag{16}$$

$M < Z < N$

$$V_Y = R_{AY} - F_{WY} \tag{17}$$

$$M_X = -R_{AY} Z + F_{WY} (Z - M) \tag{18}$$

$N < Z < L$

$$V_Y = R_{AY} - F_{WY} + F_{CY} \tag{19}$$

$$M_X = -R_{AY} Z + F_{WY} (Z - M) - F_{CY} (Z - N) + M_{WY} \tag{20}$$

For Phase II (Figure 5), the internal shearing force and bending moment were found to be:

X Component:

$O < Z < M$

$$V_X = - R_{AX} \tag{21}$$

$$M_Y = R_{AX} Z \tag{22}$$

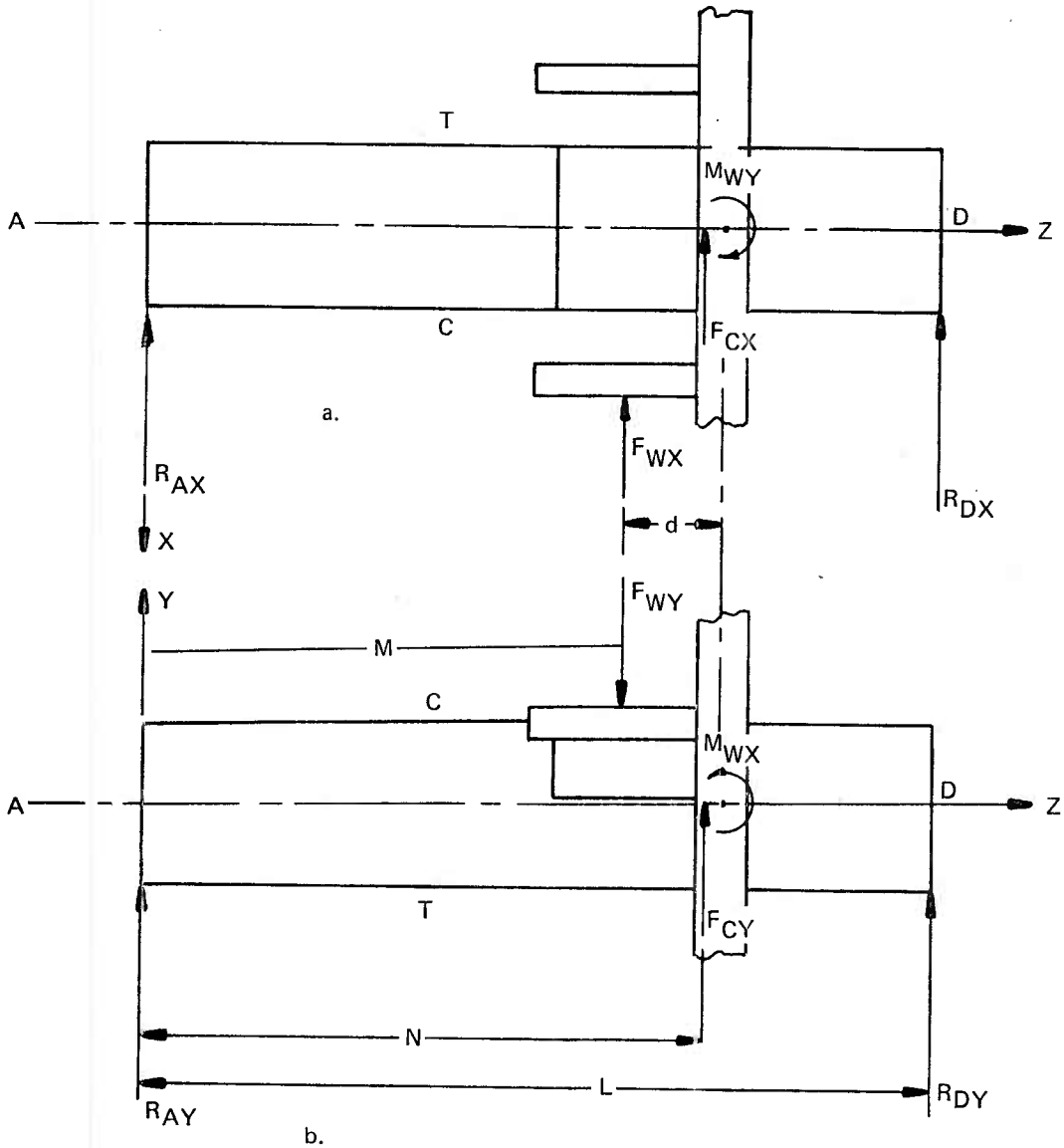

Figure 4. Loads and Reaction of Phase I: (a) Top View and (b) Side View. T and C Denote Regions of Tension and Compression, Respectively

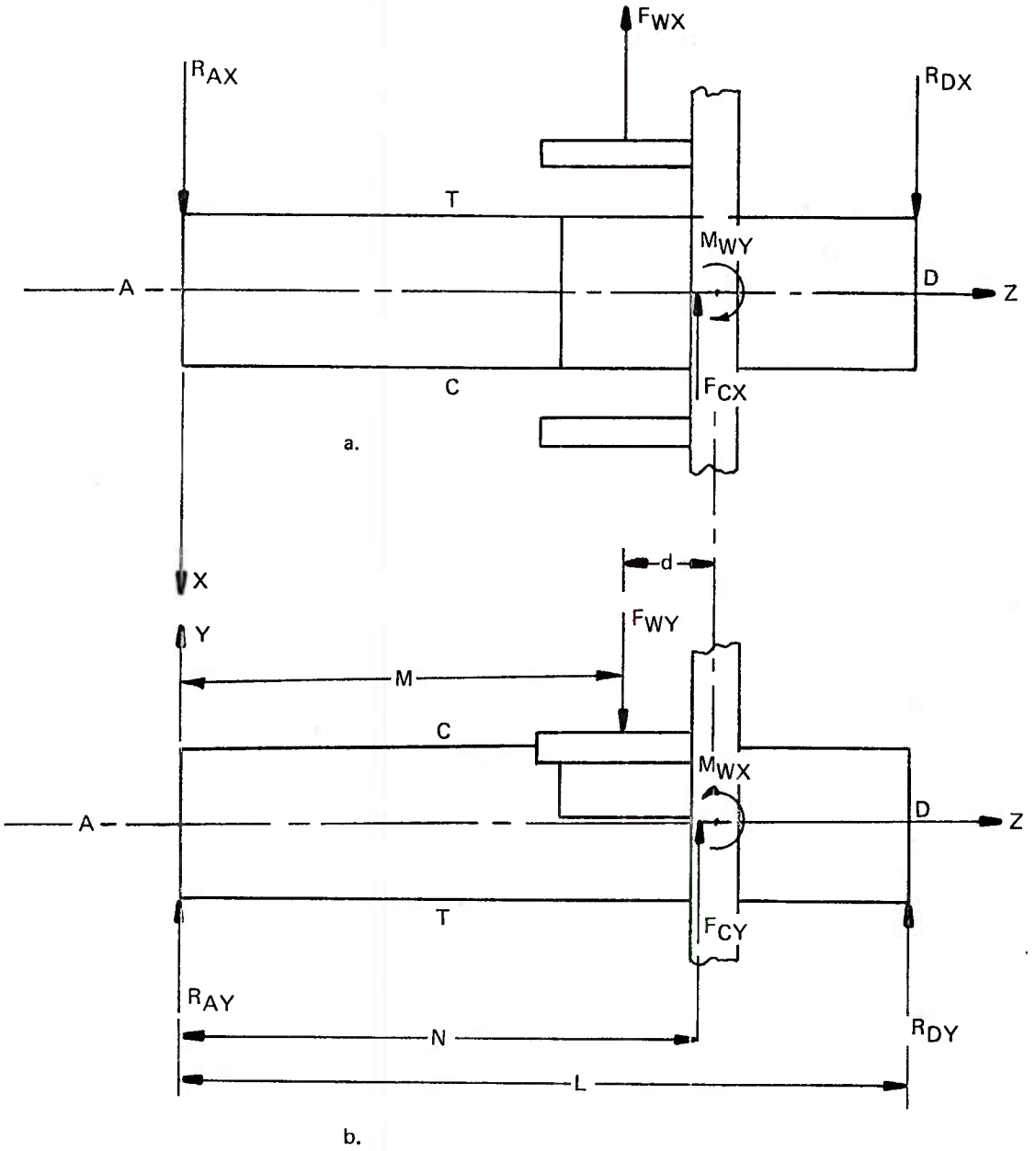

Figure 5. Loads and Reactions for Phase II: (a) Top View and (b) Side View. T and C Denote Regions of Tension and Compression, Respectively

$M < Z < N$

$$V_X = F_{WX} - R_{AX} \quad (23)$$

$$M_Y = R_{AX}Z - F_{WX}(Z - M) \quad (24)$$

$N < Z < L$

$$V_X = F_{WX} + F_{CX} - R_{AX} \quad (25)$$

$$M_Y = R_{AX}Z - F_{WX}(Z - M) - F_{CX}(Z - N) - M_{WY} \quad (26)$$

Y Component:

$O < Z < M$

$$V_Y = R_{AY} \quad (27)$$

$$M_X = -R_{AY}Z \quad (28)$$

$M < Z < N$

$$V_Y = R_{AY} - F_{WY} \quad (29)$$

$$M_X = -R_{AY}Z + F_{WX}(Z - M) \quad (30)$$

$N \quad Z < L$

$$V_Y = R_{AY} - F_{WY} + R_{CY} \quad (31)$$

$$M_X = -R_{AY}Z + F_{WY}(Z - M) - F_{CY}(Z - N) - M_{WX} \quad (32)$$

Due to the loading and reduced area at the "D" section, the maximum stress and failure occur in the "D" section. Attention was therefore restricted to this "D" section, namely, from Z = .199 in. to Z = .279 in. Using the equations given above, numerical values of V_X, V_Y, M_X and M_Y were calculated as shown in Table 3 and plotted in Figures 6 to 17. From this table and these figures, the point where the maximum moments occur are Z = .239" (Phase I) and Z = .279" (Phase II). Failure, if it occurs, would occur at these points. Therefore, it is these locations on the shaft which are used in the subsequent computation of the bending stresses.

Unsymmetric Bending

It follows from the above load analysis that the problem of stress analysis is essentially that of a shaft subjected simultaneously to bending and shear in two planes. The two planes in question are the X-Z and Y-Z planes of Figures 4 and 5.

The approach in the elastic analysis was to consider each of the bending planes separately, and then to combine their effects. M_X acting alone, will produce a bending stress, σ_1, acting on and normal to the cross-sectional area as shown in Figure 18. M_Y will produce a bending stress, σ_2 which acts on and is normal to the cross section. As seen in Figure 18, σ_2 is a linear function only of X' and is independent of Y'. Also, σ_1 is a linear function of Y' and is independent of X'. The appropriate equations are then:

$$\sigma_1 = \sigma_1(Y') = (M_X/I_{X'})\, Y' \quad (33)$$

$$\sigma_2 = \sigma_2(X') = (M_Y/I_{Y'})\, X' \quad (34)$$

Table 3. X and Y Components of Shearing Forces and Bending Moments in Slotted Section

Phase I

Case	Z, in	V_X, lb	V_Y, lb	M_X, in-lb	M_Y, in-lb
1	.199	2.635	-1.489	-.296	.524
	.239	2.635	-1.489	-.356	.630
	.279	.945	4.038	-1.95	.668
2	.199	2.563	-1.348	-.268	.510
	.239	2.563	-1.348	-.322	.613
	.279	1.246	3.247	-.192	.662
3	.199	2.526	-1.165	-.232	.503
	.239	2.526	-1.165	-.278	.604
	.279	1.448	2.155	-.192	.662

Phase II

Case	Z, in	V_X, lb	V_Y, lb	M_X, in-lb	M_Y, in-lb
1	.199	.807	-2.390	-.476	.161
	.239	.807	-2.390	-.571	.193
	.279	-2.038	2.538	-.470	.111
2	.199	1.021	-1.683	-.335	.203
	.239	1.021	-1.683	-.402	.244
	.279	-1.949	1.921	-.325	.166
3	.199	1.377	-6.843	-.136	.274
	.239	1.377	-6.843	-.164	.329
	.279	-1.616	1.334	-.111	.265

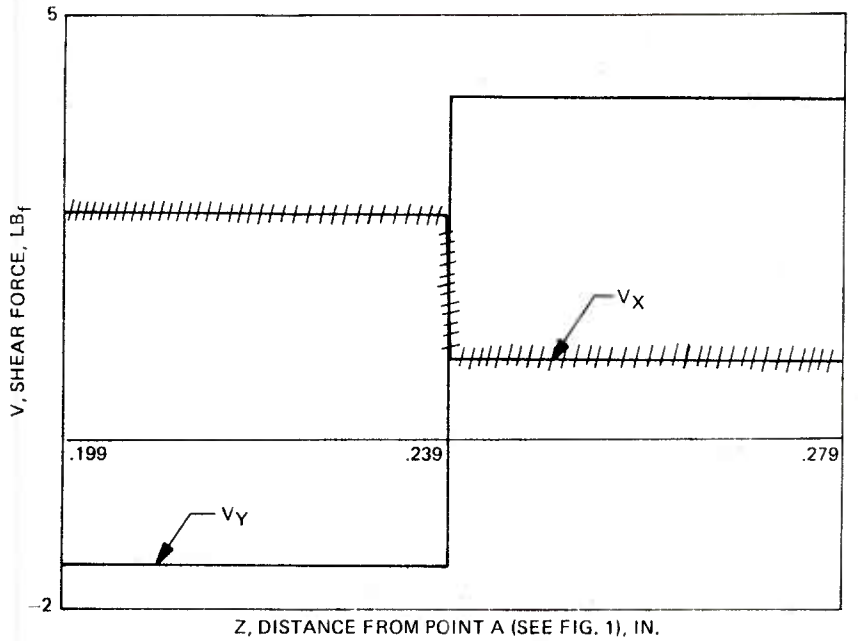

Figure 6. Shear Diagram for Phase I, Case 1.
V_X = Shear Force in the X Direction
V_Y = Shear Force in the Y Direction

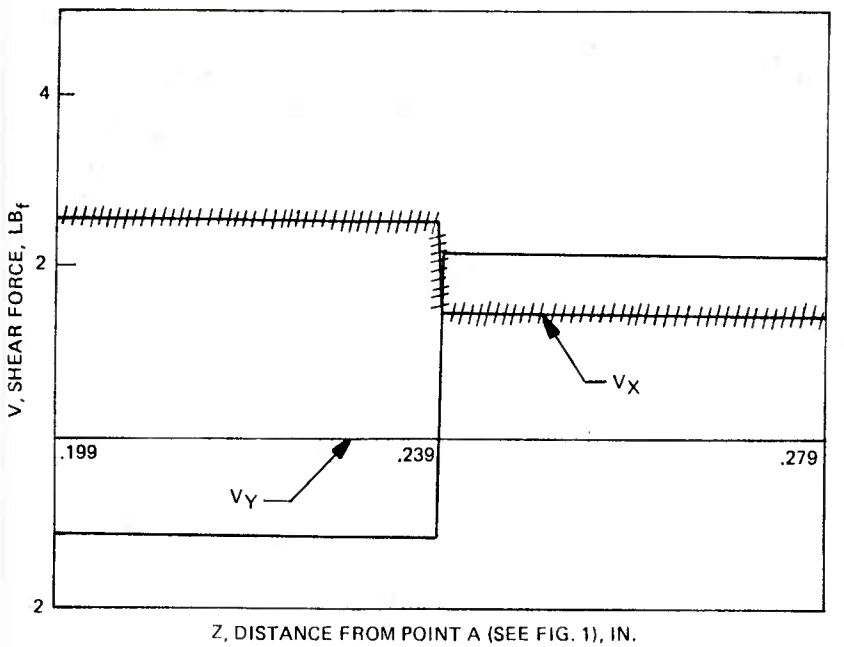

Figure 7. Shear Diagram for Phase I, Case 2.
V_X = Shear Force in the X Direction.
V_Y = Shear Force in the Y Direction.

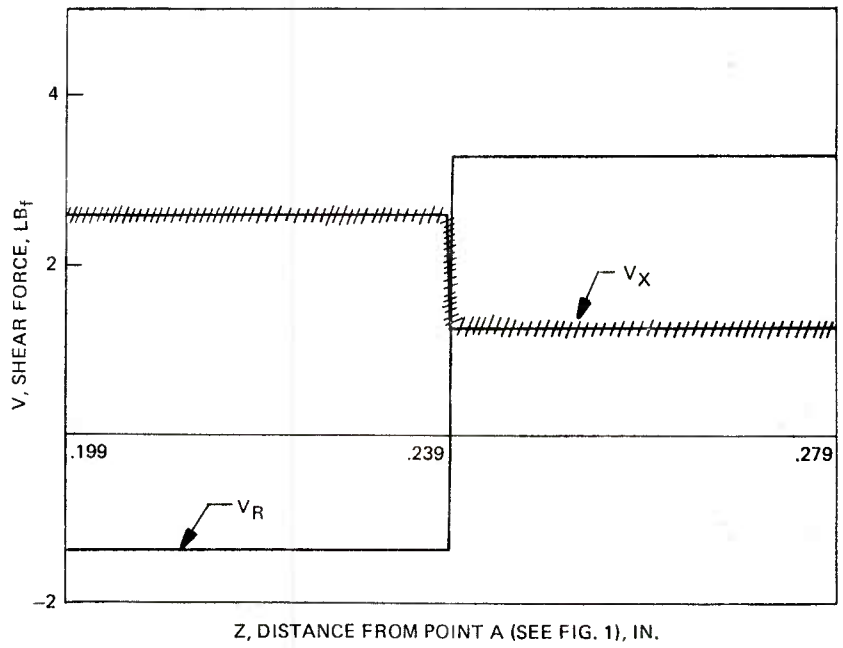

Figure 8. Shear Diagram for Phase I, Case 3.
V_X = Shear Force in the X Direction
V_Y = Shear Force in the Y Direction

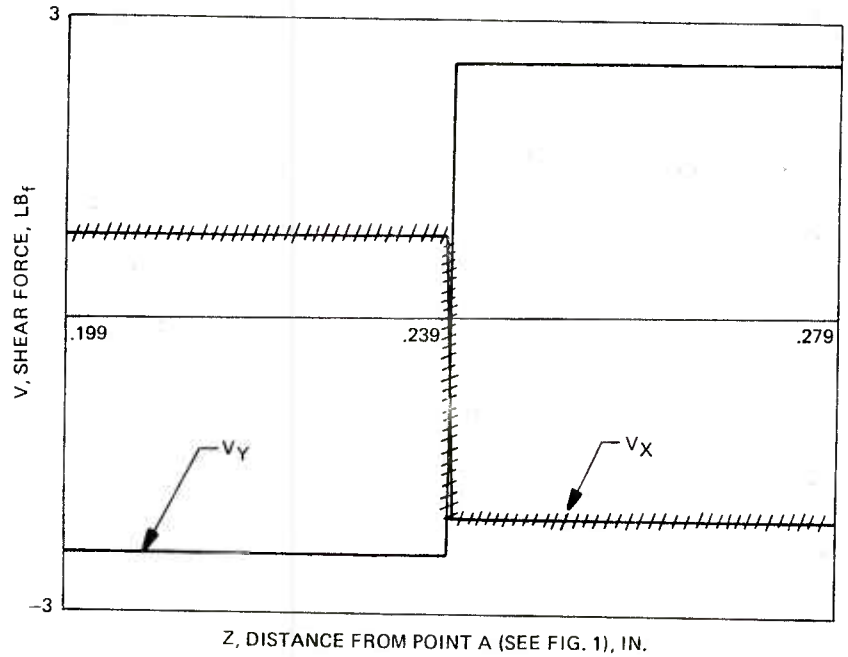

Figure 9. Shear Diagram for Phase II, Case 1.
V_X = Shear Force in the X Direction.
V_Y = Shear Force in the Y Direction.

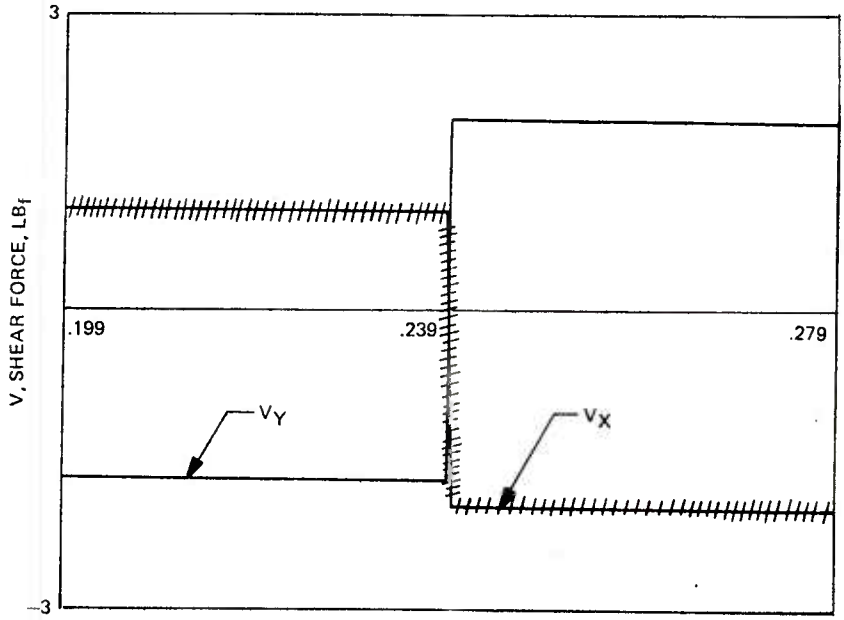

Figure 10. Shear Diagram for Phase II, Case 2.
V_X = Shear Force in the X Direction.
V_Y = Shear Force in the Y Direction.

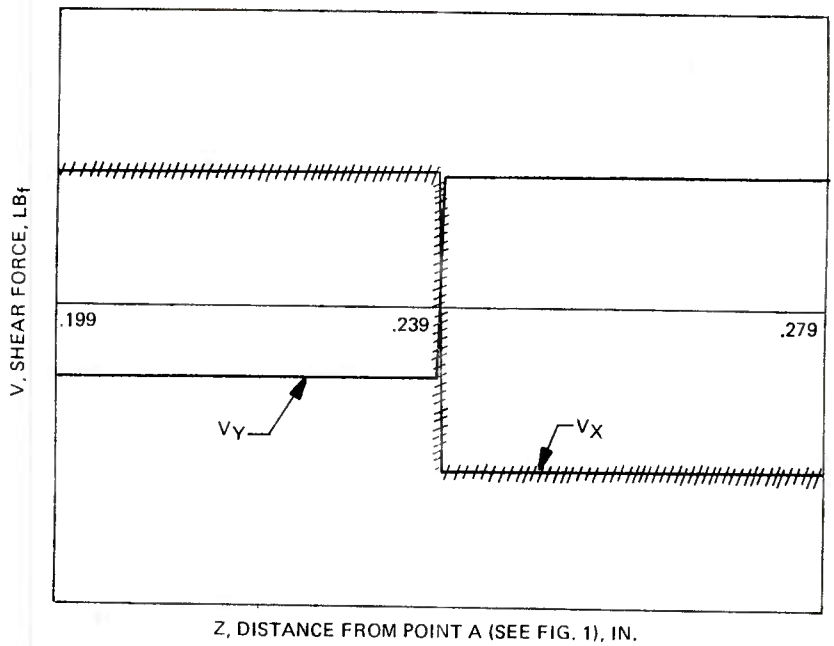

Figure 11. Shear Diagram for Phase II, Case 3.
V_X = Shear Force in the X Direction.
V_Y = Shear Force in the Y Direction.

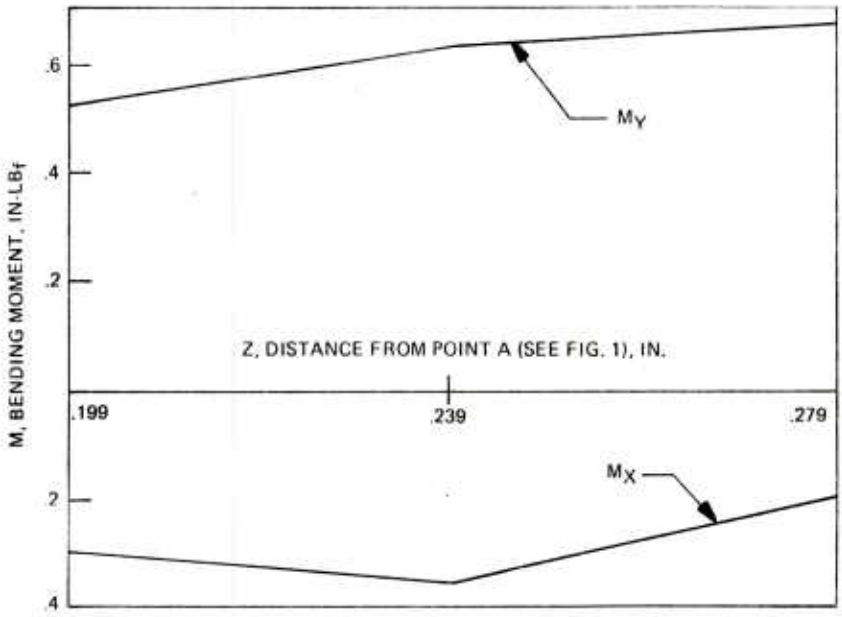

Figure 12. Moment Diagram for Phase I, Case 1.
M_X = Moment about the X Neutral Axis.
M_Y = Moment about the Y Neutral Axis.

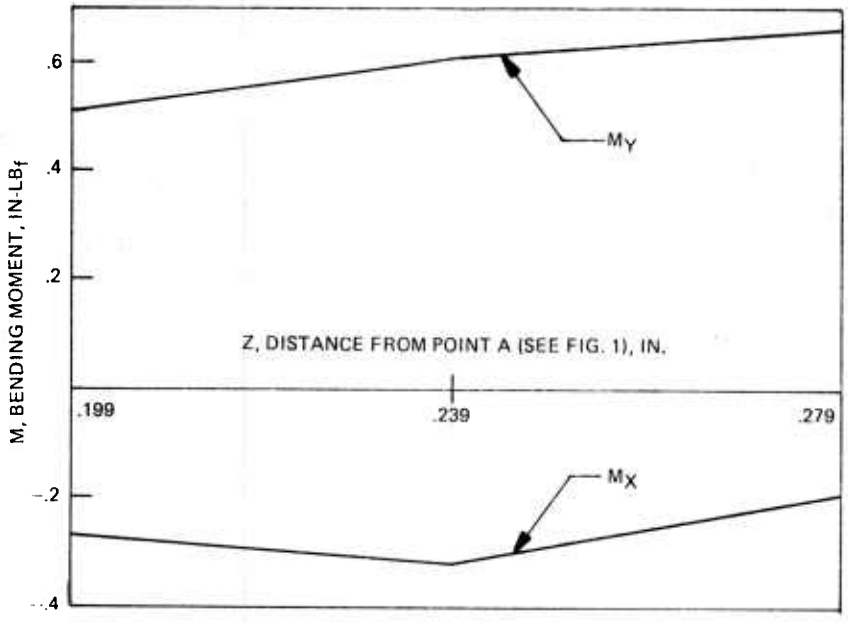

Figure 13. Moment Diagram for Phase I, Case 2.
M_X = Moment about the X Neutral Axis.
M_Y = Moment about the Y Neutral Axis.

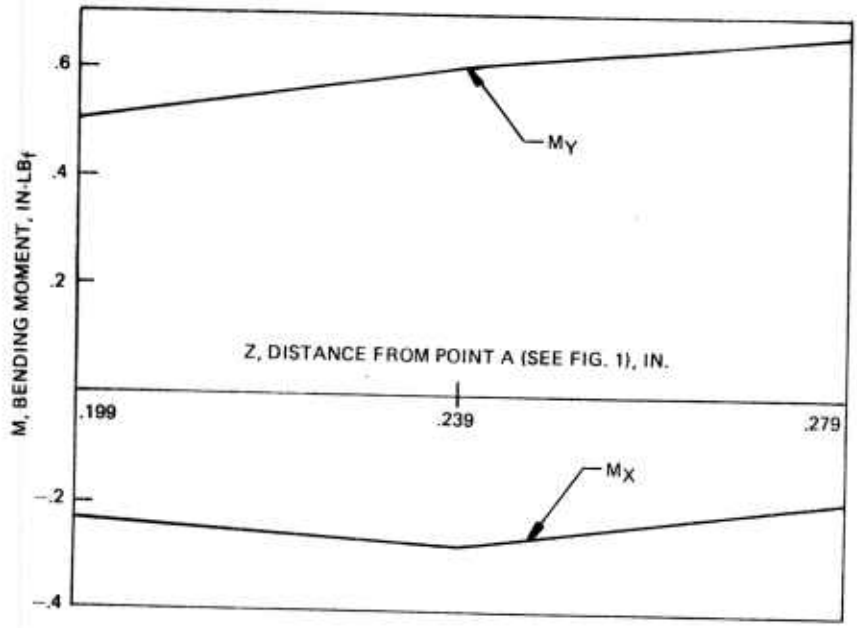

Figure 14. Moment Diagram for Phase I, Case 3.
M_X = Moment about the X Neutral Axis.
M_Y = Moment about the Y Neutral Axis.

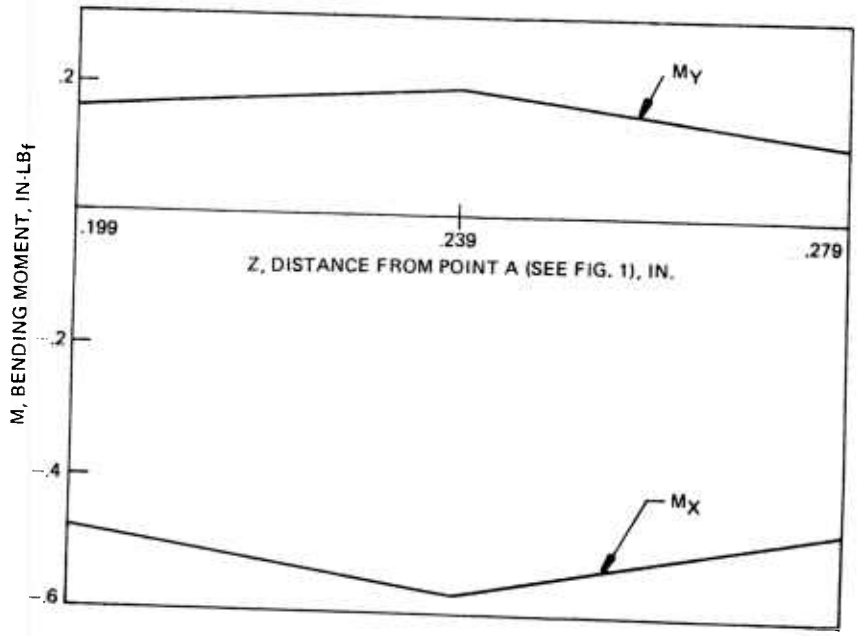

Figure 15. Moment Diagram for Phase II, Case 1.
M_X = Moment about the X Neutral Axis.
M_Y = Moment about the Y Nautral Axis.

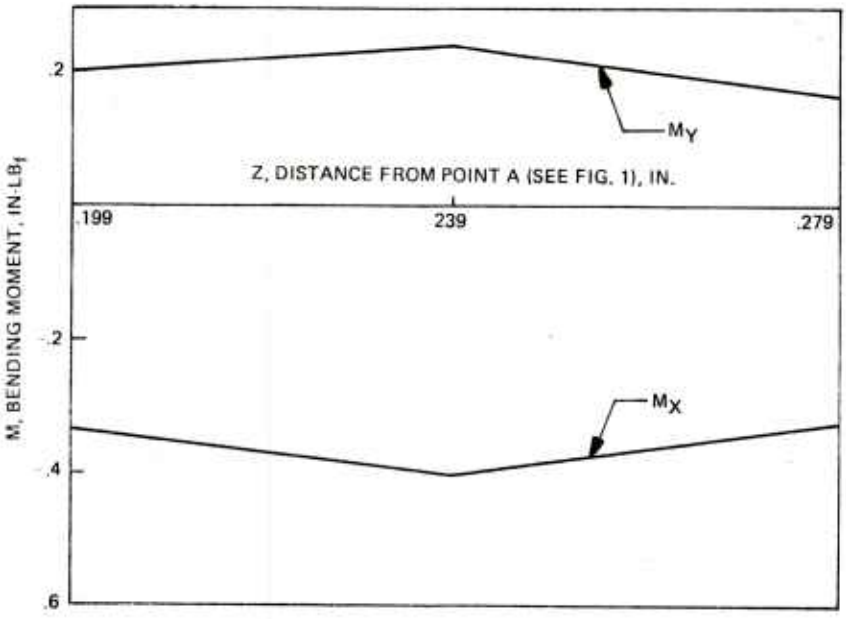

Figure 16. Moment Diagram for Phase II, Case 2.
M_X = Moment about the X Neutral Axis.
M_Y = Moment about the Y Neutral Axis.

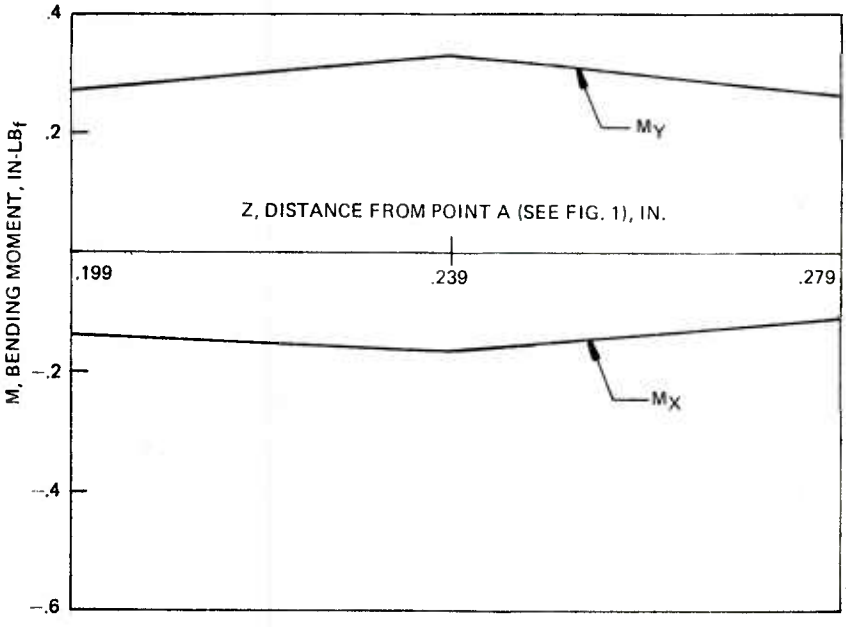

Figure 17. Moment Diagram for Phase II, Case 3.
M_X = Moment about the X Neutral Axis.
M_Y = Moment about the Y Neutral Axis.

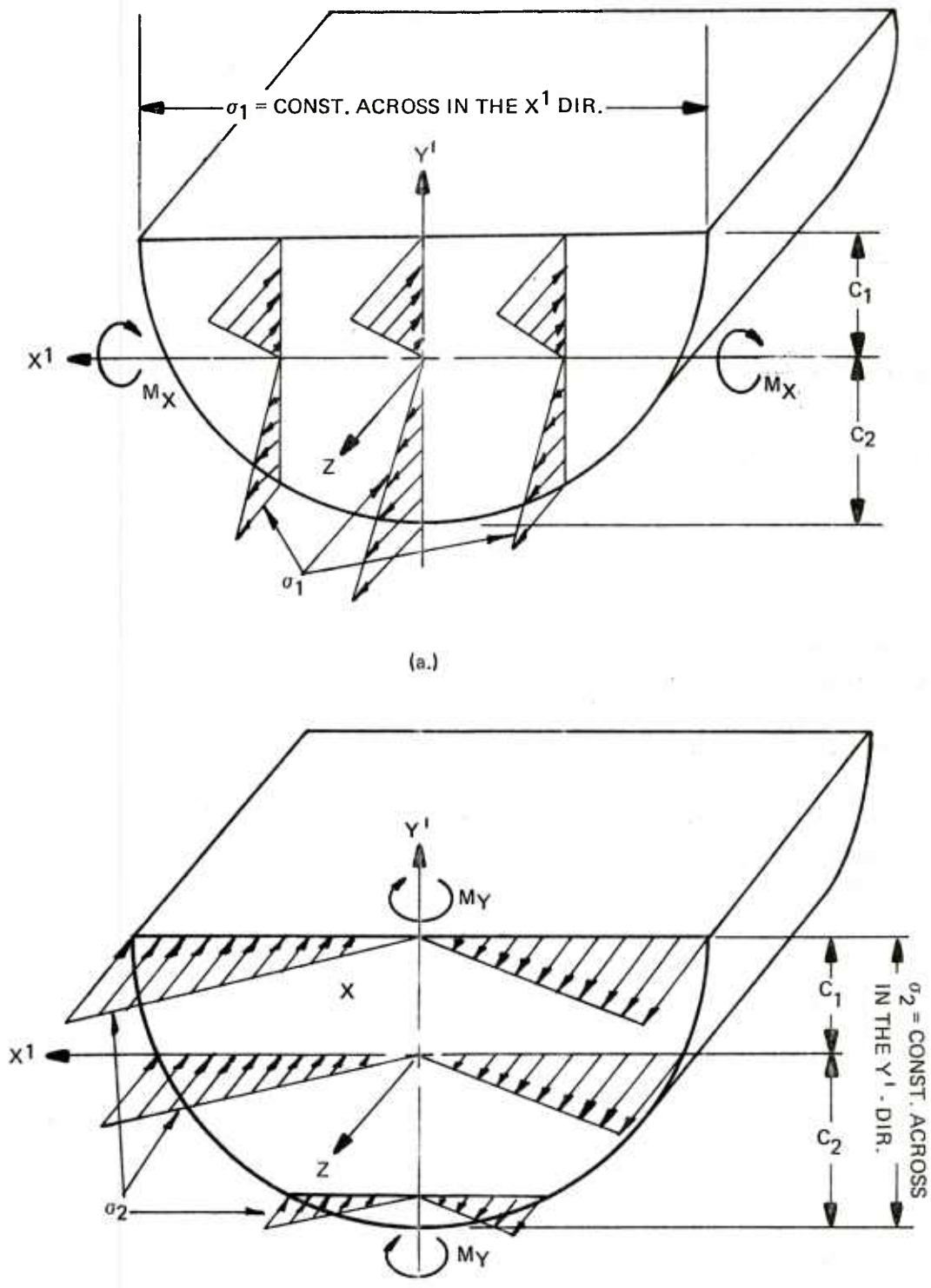

Figure 18. Individual States of Stress: (a) Stress Due to M_X and (b) Stress Due to M_Y.

$I_{X'}$ is the moment of inertia about the neutral axis X', $I_{Y'}$ is the moment of inertia about the neutral axis Y'. With respect to the drawings: 1. Y' is symmetrically located on the section. 2. the X' axis is defined by the dimensions C_1 and C_2 which have values of $C_1 = .424$ R, $C_2 = .576$ R. 3. $I_{X'}$ has a value of $0.11\ R^4$. 4. $I_{Y'}$ was calculated from the definition:

$$I_{Y'} = \int_A X^2\ dA \tag{35}$$

which resulted in

$$I_{Y'} = \pi R^4/8 \tag{36}$$

The total stress is the sum of the individual components, σ_1 and σ_2. Examination of Figure 18 and Equations 33 and 34 show that the total loading, σnom, will result in a complex stress distribution. This is indicated, schematically, in Figure 19. Figure 19 shows the sum of the two distributions. The stress σ_1, about the X' axis caused a tensile (T) and compressive (C) region. The stress σ_2 about the Y' axis also causes tensile and compresive regions. Upon addition, the four regions can be identified CC, CT, TC, and TT. The symbols denote the contribution from each stress. For example CC denotes that in Region 1 both σ_1 and σ_2 were compressive.

Tables 4 and 5 contain the numerical values of the total stress distribution, $\sigma_1 + \sigma_2$, for a large number of interior and boundary points which are identified in Figure 20. Both interior and exterior points were examined for each loading case within each Phase. For all six loading conditions the tables show clearly that:

1. The maximum compressive stress always occured at point D.
2. The maximum tensile stress was at either point J or M. Note that the maximum stress occurs always at the boundary rather than at the interior. This is intuitively reasonable since it parallels the simpler uni-plane bending of elementary beam theory.
3. The maximum stress occurs in Phase I, case 1, it is compressive, and has a value of 103 ksi. Maxima for all other cases are underlined. The influence of the shear stress on the total stress distribution was considered. The shear stress, τ_{XY}, is given approximately by

$$\tau \cong V/A \tag{37}$$

where V is the shear force and A the cross sectional area. Table 6 presents these stresses for both (X and Y) components of the shear force. The values of V were taken from Table 3. As can be seen, the maximum shear stress is of the order of 3 ksi and is negligible compared to the bending stresses.

Plastic Flow and Failure

Consider the circular beam of Figure 21. The Von-Mises criterion for incipient flow is:

$$\sigma^2 + 3\tau^2 = 3k^2 \tag{37}$$

where σ is the normal stress, τ the shear stress and k is the yield stress in simple shear.

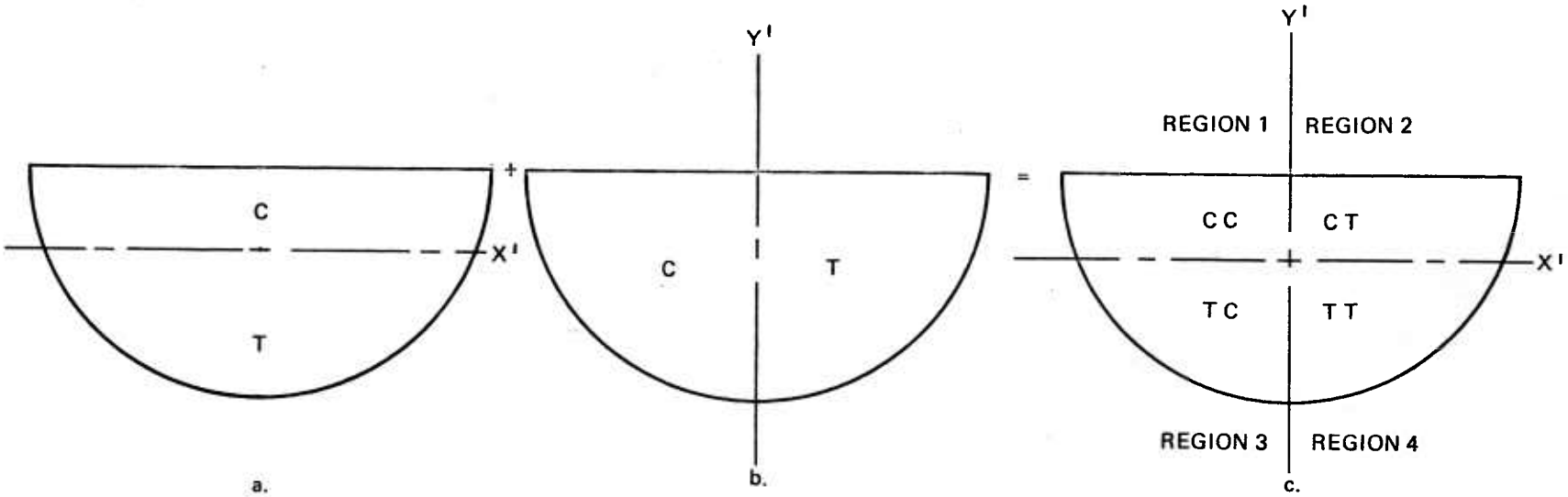

Figure 19. Combined States of Stress.
a - Bending in the Y-Z Plane.
b - Bending in the X-Z Plane
c - Equivalent Bending Effect of b and c.

Table 4. Combined Bending Stress at Different Points of Cross Section for Phase I

Interior Points	Combined Stress ksi Case 1	2	3	Exterior Points	Combined Stress ksi Case 1	2	3	
11	25	24	23	A	61	56	51	
12	36	34	31	B	76	71	65	
13	46	43	39	C	90	86	80	
21	40	39	37	D	103	98	93	
22	51	48	46	E	89	85	81	Compression
23	61	58	54	F	77	75	72	
31	55	53	52	G	65	60	62	
32	65	63	60	H	52	52	52	
33	76	72	68	-	-	-	-	
44	32	30	32	I	63	57	49	
45	57	52	56	J	69	63	56	
54	39	37	39	K	74	68	61	
55	64	59	64	L	76	71	64	Tension
64	47	44	46	M	76	72	66	
65	71	66	71	N	74	70	65	
74	54	51	54	O	67	64	62	
84	61	59	68	P	52	52	51	

Table 5. Combined Stress at Different Points of Cross Section for Phase II

Interior Points	Combined Stress ksi Case 1	2	3	Points	Combined Stress ksi Case 1	2	3	
11	21	17	12	A	71	58	28	
12	38	29	17	B	83	63	36	
13	55	41	22	C	87	68	43	
21	25	23	19	D	91	73	49	
22	42	35	24	E	68	53	43	Compression
23	59	46	29	F	51	45	37	
31	30	28	27	G	33	32	32	
32	47	40	31	H	16	20	26	
33	63	52	36	-	-	-	-	
44	42	30	15	I	101	71	29	
45	81	58	26	J	101	72	32	
54	44	33	19	K	99	72	34	
55	83	61	30	L	93	69	36	Tension
64	46	36	22	M	84	64	36	
65	85	64	33	N	70	55	35	
74	48	41	26	O	49	42	32	
84	50	44	29	P	16	19	26	

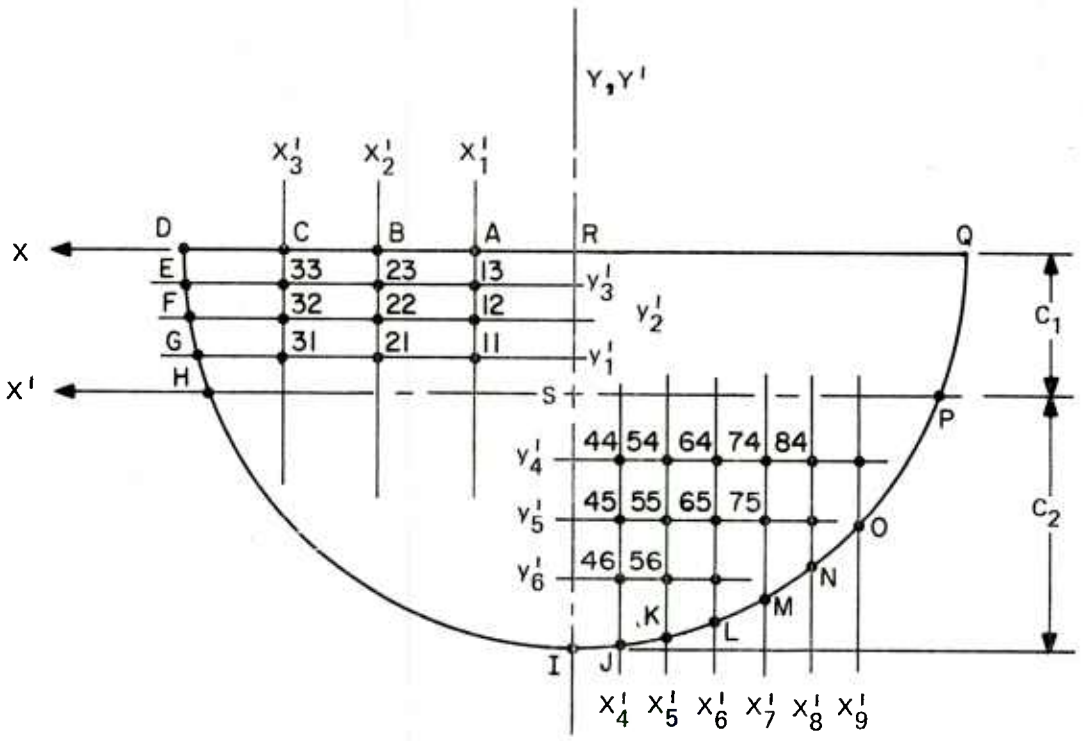

X'_1 = .008 IN.

X'_2 = .016 IN.

X'_3 = .024 IN.

X'_4 = .004 IN.

X'_5 = .008 IN.

X'_6 = .012 IN.

X'_7 = .016 IN.

X'_8 = .020 IN.

X'_9 = .024 IN.

Y'_1 = .003 IN.

Y'_2 = .006 IN.

Y'_3 = .009 IN.

Y'_4 = .007 IN.

Y'_5 = .014 IN.

Y'_6 = .016 IN.

Figure 20. Locations of Points used in Calculations

Table 6. Maximum Average Shearing Stress in the Flat Section

Phase I		
Case	T_{XY_1}, psi	T_{XY_2}, psi
1	1746	2675
2	1698	2151
3	1673	1427
Phase II		
Case	T_{XY_1}, psi	T_{XY_2}, psi
1	1350	1681
2	1291	1272
3	1070	884

T_{XY_1} = Shear stress due to X component of shear force.

T_{XY_2} = Shear stress due to Y component of shear force.

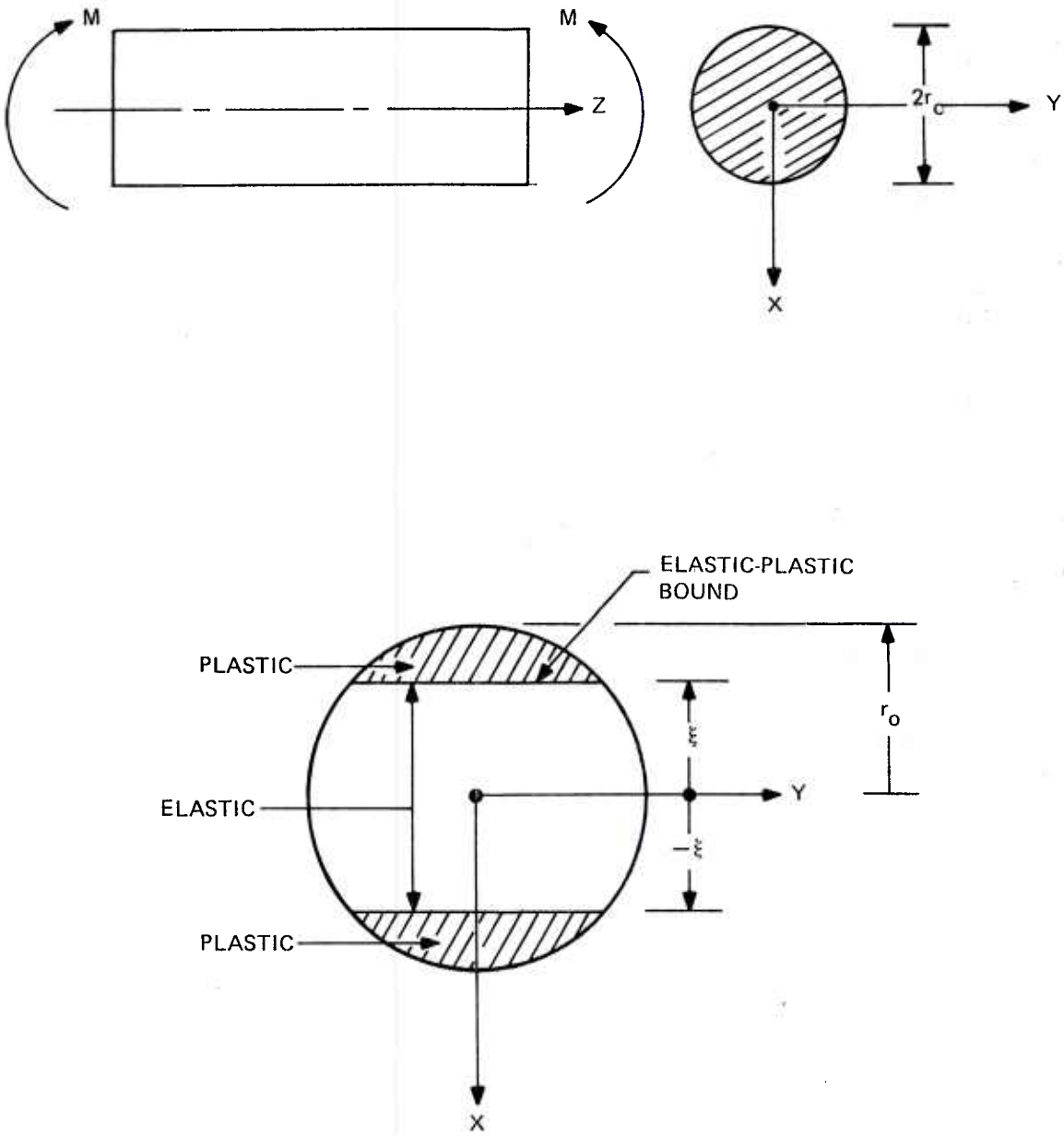

Figure 21. State of Stress

Since the shear stress is much smaller than the normal stress, i.e.,

$$|\tau| \ll |\sigma| \tag{38}$$

the yield condition, Equation 37 is:

$$\sigma = \pm k \cdot \sqrt{3} \tag{39}$$

To establish conditions incipient for flow one must consider the elastic behavior just before plasticity commences.

The relation between stress and bending moment for an elastic beam is:

$$\sigma = M_X/I \tag{40}$$

Since $\frac{M}{I}$ is a constant at a particular section, it follows from Equation 40 that elastic stress is a maximum at the outer fibers. Thus plasticity commences there first.

Thus, using Equations 39 and 40, the critical moment, M_c, at which plasticity begins at the outer fiber is:

$$M_c = \sqrt{3} k \, I/r_o \tag{41}$$

For moments smaller than M_c the beam is elastic and, disregarding the question of stress concentration, does not fail. It is important to note that M_c is a property inherent to the beam since its value depends only on material and geometric constants.

The value of the shear yield, k, is most conservatively related to the Tresca criterion as:

$$k = (1/2)\sigma_Y \tag{42}$$

where σ_y is the tensile yield strength of the metal.

Thus the critical moment is:

$$M_c = (\sqrt{3}/2) \sigma_Y \, I/r_o \cong .87 \, \sigma_y \, I/r_o \tag{43}$$

and since:

$$I = \pi r_0^4/4 \tag{44}$$

$$M_c \cong .68 \, r_0^3 \, \sigma_Y \tag{45}$$

It is important to note that while M_c causes plastic flow in the outer fibers, the remainder of the beam is elastic.

Failure occurs when the moment exceeds the critical value by an amount to make part of the crosssection plastic. An upper limit on this value, M_f, is found in the analysis below.

Consider the section shown in Figure 21. Plasticity commences, as noted above, when $|\xi| = r_o$, at the outer fibers. As M is increased, more of the beam becomes plastic. This occurs as $|\xi|$ decreases. When $\xi = o$, and the section is entirely plastic, the beam is permanently deformed and therefore failed.

The state of stress for each region of the beam section is:

$$\begin{aligned} \sigma &= k\sqrt{3} && \text{for} && -r_0 \leqslant Z \leqslant -\xi \\ \sigma &= kZ\sqrt{3}/\xi && \text{for} && -\xi \leqslant Z \leqslant \xi \\ \sigma &= k\sqrt{3} && \text{for} && \xi \leqslant Z \leqslant r_o \end{aligned} \tag{46}$$

By definition the moment caused by the stress system, Equation 46 is:

$$M = \int_{-r_o}^{r_o} \sigma(Z)\ Z\ dA = M(\xi) \tag{47}$$

where dA is an area element. Noting the symmetry of deformation about the Y-axis, Equation 47 is:

$$M = 2\int_{r_\xi}^{r_o} \sigma\ (Z)\ Z\ dA + 2\int_{o}^{\xi} \sigma\ (Z)\ Z\ dA, \tag{48}$$

recalling that:

$$dA = 2\ (r_o^{\,2} - Z^2)^{1/2}\ dZ, \tag{49}$$

and also the values of $\sigma(Z)$ given by Equation 46, the final integrated result is:

$$\begin{aligned} M(\xi)/2 = {} & (2/3)\ k\sqrt{3}\left[r_o^{\,2} - \xi^{\,2}\right]^{3/2} + \\ & + Z\ k\sqrt{3}\left[-(r_o^{\,2} - \xi^{\,2})^{3/2}/4 + r_o^{\,2}(r_o^{\,2} - \xi^{\,2})^{1/2}/8 + \right. \\ & \left. + (r_o^{\,4}/8\,\xi)\ \sin^{-1}\ (\xi/r_o)\right] \end{aligned} \tag{50}$$

The value of M_f, an upper limit to the moment which causes complete failure, is obtained by allowing ξ to approach zero in Equation 50 . The result is:

$$M_f = 1.155\ \sigma_Y\ r_o^{\,3} \tag{51}$$

Comparing this value to M_c in Equation 45 it is seen that, theoretically, when M_c is exceeded by about 70%, the beam is completely failed. In the present application, however, where virtually no plastic flow and permanent deflection are permitted, this factor of 70% beyond M_c is too great for design allowance. Also, the real cross-section is a half circle and not a complete circle as assumed. While a value for M_f for a half-circle has not been attempted, it is obvious that M_f will certainly not be greater than M_c.

DISCUSSION AND CONCLUSION

The maximum stress found in the elastic analysis with no stress concentration factor was 103 ksi. The yield stress of the beam material is 120 ksi. The right angle formed by the machined flat will introduce a stress concentration factor. Since any stress concentration factors will elevate the stress to well beyond 120 ksi, which is the yield strength of the material, it is concluded that the beam is on the verge of ductile, plastic failure.

REFERENCES

1. L. Farace, "Runaway Escapement Redesign M125A1 Modular Booster", Tech. Report FA-TR-74045, 1974.

2. S. Timoshenko and G. H. MacCullough, "Elements of Strength of Materials", 1949.

DISTRIBUTION

Commander
US Army Materiel Development & Readiness Command
5001 Eisenhower Avenue
Alexandria, VA 22333

1 Attn: DRCDMD

1 Attn; DRCDMR

1 Attn: DRCDMD-T

1 Attn: DRCD-I,
Foreign Science & Technology Division

1 Attn: DRCDE-W

1 Attn: DRCMT,
L. Croan

1 Attn: DRCDE-DE,
E. Lippi

Commander
US Army Armament Command
Rock Island, IL 61201

1 Attn: Technical Information Div.

1 Attn: DRSAR-RD,
Mr. J. Brinkman

1 Attn: DRSAR-RDG-A,
J. Williams

1 Attn: PM, CAWS,
H. Noble

Commander
Rock Island Arsenal
Attn: Technical Information Div.
Rock Island, IL 61202

Commander
Aberdeen Proving Ground
Attn: STEAP-TL, Technical Library
Aberdeen, MD 21005

Commander
US Army Materials & Mechanics Research Center
Watertown, MA 02171

1 Attn: DMXMR,
Dr. E. Wright

1 Attn: Technical Information Div.

Commander
Picatinny Arsenal
Dover, NJ 07801

1 Attn: PM,
Selected Ammunition

1 Attn: SARPA-FR-M,
Chf, Materials Eng. Div.

1 Attn: SARPA-AD

1 Attn: Technical Information Div.

Commander
Watervliet Arsenal
Watervliet, NY 12189

1 Attn: SARWV-RDR,
Dr. T.E. Davidson

1 Attn: Technical Information Div.

Commander
US Army Research Office
P.O. Box 12211
Attn: Dr. George Mayer, Director
Metallurgy & Materials Science Division
Research Triangle Park, NC 27709

Commander
Naval Air Development Center
Johnsville, Aero Materials Dept.
Attn: Mr. Forrest Williams
Warminister, PA 18974

DISTRIBUTION (Cont)

Director
Air Force Materials Laboratory
Attn: AFML, Technical Library
Wright-Patterson AFB
Dayton, OH 45433

Director
National Academy of Science
Attn: Materials Advisory Board
2101 Constitution Avenue, N.W.
Washington, DC 20418

Metals & Ceramic Information Center
Battelle Memorial Institute
505 King Avenue
Columbus, OH 43201

US Atomic Energy Commission
Document Library
Germantown, MD 21403

Director
US Army Air Mobility Research & Development Laboratory
Ames Research Center
Attn: Mr. Paul Yaggy
Moffet Field, CA 94035

Commander
US Army Mobility Equipment Research & Development Command
Attn: STSFB-MMM, Mr. W. Baer
Ft. Belvoir, VA 22060

Commander
Redstone Arsenal
Attn: Technical Information Div.
Huntsville, AL 35809

Commander
Rocky Mountain Arsenal
Attn: Technical Information Div.
Denver, CO 80240

Commander
US Army Natick Research & Development Command
Attn: Technical Information Div.
Natick, MA 07160

Commander
Harry Diamond Laboratories
2800 Powder Mill Road
Attn: AMXDO-TIB
Adelphi, MD 20783

Commander
Naval Air Systems Command
Department of the Navy
Attn: AIR 5203, Mr. R. Schmidt
Washington, DC 20361

Commander
Naval Ships Systems Command
Department of the Navy
Attn: Code 03423
Washington, DC 20025

Commander
Office of Naval Research
Department of the Navy
Attn: Code 423
Washington, DC 20023

Commander
US Army Foreign Science & Technology Center
Attn: Mr. William F. Marley
220 7th Street N.E.
Charlottesville, VA 22901

Commander
US Naval Weapons Laboratory
Attn: Technical Information Div.
Dahlgren,VVA 22448

Commander
US Naval Engineering Experimental Station
Attn: WCTRL-2, Materials Lab.
Annapolis, MD 21402

DISTRIBUTION (Cont)

Commander
Air Research & Development Command
Andrews Air Force Base
Attn: RDRAA
Washington, DC 20025

Commander
US Naval Ordnance Laboratory
Attn: Code WM
Silver Spring, MD 20910

Commander
Aeronautical Systems Division
Wright-Patterson Air Force Base
Attn: Technical Information Div.
Dayton, OH 45433

Director
US Army Advanced Materials Concept Agency
Attn: Technical Information Div.
2461 Eisenhower Avenue
Alexandria, VA 22314

Director
US Naval Research Laboratory
Attn: Mr. W.S. Pellini, Code 6300,
Metallurgy Div.
Washington, DC 20390

Director
Naval Ships Research & Development Center
Attn: Mr. Abner R. Willmer,
Chief of Metals Research
Bethesda, MD 20034

Director
Air Force Armament Laboratory
Attn: AFATL/DLOSL
Eglin AFB, FL 32542

Director
Air Force Weapons Laboratory
Attn: Technical Information Div.
Kirtland AFB, NM 87118

Director
Air Force Materials Laboratory
Wright-Patterson Air Force Base
Dayton, OH 45433

1 Attn: AFML/LLD,
Dr. T.M.F. Ronald

1 Attn: AFML,
Technical Library

Director
Defense Advanced Research Projects Agency
Attn: Dr. E.C. Van Reuth
1400 Wilson Boulevard
Arlington, VA 22209

Director
National Academy of Science
Attn: Materials Advisory Board
2101 Constitution Avenue, N.W.
Washington, DC 20418

Director
National Aeronautics & Space Administration
Attn: Code RRM
Federal Building #10
Washington, DC 20546

Director
National Bureau of Standards
Attn: Technical Information Div.
Washington, DC 20025

Federal Aviation Administration
Attn: Administrative Standard Div.
800 Independence Avenue, S.W.
Washington, DC 20690

Chief, Bureau of Ships
Department of the Navy
Attn: Code 343
Washington, DC

DISTRIBUTION (Cont)

Chief, Bureau of Aeronautics
Department of the Navy
Attn: Technical Information Div.
Washington, DC

Chief, Bureau of Weapons
Department of the Navy
Attn: Technical Information Div.
Washington, DC 20025

Mr. Robert H. Brown
1411 Pacific Avenue
Natrona Heights, PA 15065

Dr. Robert S. Busk
3606 Windsor Court
Midland, MI 48640

Mr. J.B. Hess
Kaiser Aluminum & Chemical Corp.
Aluminum Division Research Center
for Technology
P.O. Box 870
Pleasanton, CA 94566

Dr. Schrade Radtke
International Lead Zinc Institute
292 Madison Avenue
New York, NY 10017

Prof. M.C. Flemings
Department of Metallurgy
Materials Science
Mass. Institute of Technology
Cambridge, MA 02139

Mr. Carson L. Brooks
Reynolds Metal Company
4th & Canal Streets
Richmond, BA 23219

Mr. Harold Hunsicker
Aluminum Company of America
Alcoa Technical Center
Alcoa Center, PA 15069

Dr. E.J. Ripling
Materials Research Laboratory, Inc.
1 Science Road
Glenwood, IL 60425

Dr. Thomas E. Leontis
Battelle, Columbus Laboratories
505 King Avenue
Columbus, OH 43201

Defense Documentation Center (12)
Cameron Station
Alexandria, VA 22314

Commander
Frankford Arsenal
Philadelphia, PA 19137

1 Attn: AOA-M

1 Attn: TD

1 Attn: CE

1 Attn: QAA-R

1 Attn: PA

1 Attn: GC

1 Attn: PD,
Mr. D. Rosenblatt

1 Attn: PDM,
Mr. George White

3 Attn: PDM,
Mr. J.D. Corrie

1 Attn: PDM-P

10 Attn: PDM-E/64-4.
Mr. P. Gordon

10 Attn: PDM-E,
Mr. F. Lee

DISTRIBUTION (Cont)

Frankford Arsenal (Cont)

1 Attn: PDM-E,
Project File

1 Attn: PDM-A

1 Attn: PDR,
Mr. H. Kahn

10 Attn: PDM-E,
Mr. M. Schwartz

1 Attn: MD

1 Attn: MDA

1 Attn: MDA-D

1 Attn: MDA-D,
Mr. K. Ryan

1 Attn: MDA-D,
Mr. D. Lenton

1 Attn: MDA-D,
Mr. K. Pitko

1 Attn: MDA-E,
Mr. L. Farace

1 Attn: MDC

1 Attn: MDC-A,
Mr. F. Shinaly

1 Attn: MDM

1 Attn: MDS

1 Attn: MDS-S

1 Attn: FI

1 Attn: MT

Frankford Arsenal (Cont)

1 Attn: MTT

3 Attn: TSP-L,
1 - Reference Copy
1 - Circulation Copy
1 - Technical Reports Editing

Printing & Reproduction Division
FRANKFORD ARSENAL
Date Printed: 28 Sept. 1976